AIAA 81-0675R

Microwave Plasma Generation of Hydrogen Atoms for Rocket Propulsion

R. Chapman,* J. Filpus,* T. Morin,* R. Snellenberger,* J. Asmussen,† M. Hawley,‡ and R. Kerber§
Michigan State University, East Lansing, Michigan

Hydrogen dissociation in a microwave plasma and recombination is under study for propulsion. The species and energy transport and reaction processes occurring in a microwave discharge are investigated. A general model of the reaction system has been developed which supports experiment design and data correlation. The energy efficiency of the dissociation-recombination cycle is considered. Models of the recombination process are being developed to include estimates of rotational and vibrational energies, the effect of molecular relaxation on thermal energy, and the effect of bulk kinetic energy of flow on total energy of reaction, so as to avoid thermal equilibrium limitations. It was found that system pressure is an important parameter.

Nomenclature

A = cross-sectional area for flow, m^2
a = rate constant parameter 1, kgmole^{-2} m^6 s^{-1} T^{-6}
b = rate constant parameter 2 (dimensionless)
c = rate constant parameter 3 = (activation energy/R), K
C_p = heat capacity at constant pressure, J kgmole^{-1} K^{-1}
E = electric field, V m^{-1}
F_{H_2} = inlet hydrogen flow rate
g_c = gravitational constant, m^2 s^{-2} J^{-1}
ΔH = heat of reaction, J kgmole^{-1}
k = rate constants
K_{eq} = equilibrium constant, m^3 kgmole^{-1}
m_0 = molecular weight of hydrogen, kg·kgmole^{-1}
N_A = Avogadro's number
N = number density = PN_A/RT, m^{-3}
P = pressure, Pa
P_{abs} = power absorbed, W
R = gas constant, 8314J kgmole^{-1} K^{-1}
$\mathfrak{R}$ = reaction rate, kgmole m^{-3} s^{-1}
T = temperature, K
u_b = bulk flow velocity, m s^{-1}
V = volume of NOCl reservoir, m^3
X = conversion
z = distance down reactor, m
[ ] = concentration of species, kgmole m^{-3}

Introduction

HYDROGEN atom recombination reactions have potential as an important alternative for rocket propulsion. Previous studies[1-3] have acknowledged the importance of the propulsion concept but have concentrated on production of atoms on Earth and storage in the solid state. Recently, a research program was initiated to investigate the feasibility of efficient onboard hydrogen atom generation followed by recombination for spacecraft propulsion. Several methods—namely, photolysis and electron pulse radiolysis, thermal dissociation, direct-current discharges, and alternating-current discharges—were considered for dissociating molecular hydrogen to produce hydrogen atoms. A microwave plasma system was selected as a promising, energy-efficient method for hydrogen atom generation because of literature data reporting high conversions of hydrogen and because of the expected high coupling between the source and the gas.[4,5] The major thrust of this present work is on the optimization of reaction conditions for maximizing conversion of hydrogen to atoms in microwave plasmas.

Even though the major emphasis is on atom generation, it is necessary to consider recombination to understand effects of variables since recombination processes occur both in the plasma and downstream zones. Pressure is an important process variable because atom generation is favored at low pressure whereas recombination is favored at high pressure. Equilibrium constraints are strong functions of both temperature and pressure. Theoretical considerations of reactions and thermodynamics are presented for both the plasma and recombination zones.

The experimental facility is a flow microwave plasma reaction system. The goal of the experimental work is to obtain data on conversion of hydrogen to hydrogen atoms as a function of microwave plasma reaction parameters, such as pressure, power density, cavity tuning, cavity mode, and time in the plasma zone. The microwave cavity design is based on that described by Mertz.[6,7] Hydrogen atom concentration is measured just downstream from the plasma by NOCl titration.

Extensive modeling of the plasma and recombination zones is done. In addition, the thermodynamics and kinetics of recombination are treated in detail in order to provide understanding as to the conversion of energy of recombination to kinetic energy of the gas.

Concept and Background

Atomic hydrogen has long been seen as a desirable rocket fuel. The comparatively large amount of energy (104.2 kcal/gmole) released in the recombination reaction $2H \rightarrow H_2$ and the low mass of the reaction products promise theoretical exhaust velocity and specific impulse greater than any other chemical rocket.

Table 1 lists the specific impulse for several of the propellants currently in use, for two propulsion systems under development, and for atomic hydrogen with various fractions dissociated. Even 10% dissociation gives a specific impulse comparable to the NERVA. With high efficiency the atomic hydrogen rocket, at total dissociation, might rival the ion

Presented as Paper 81-0675 at the AIAA/JSASS/DGLR 15th International Electric Propulsion Conference, Las Vegas, Nev., April 21-23, 1981; submitted April 28, 1981; revision received April 12, 1982.

*Research Assistant, Department of Chemical Engineering.
†Professor, Electrical Engineering and Systems Science.
‡Professor, Chemical Engineering.
§Professor, Mechanical Engineering and Associate Dean of Engineering.

Table 1 Specific impulse for various propellants

Propellant	Specific impulse, s	Reference
O_2-kerosene	300	7
O_2-H_2	391	7
N_2O_4-UDMH-Hydrazine	278	7
Nuclear (NERVA)	825	7
Ion	1500-8000	7
Atomic hydrogen		
H:H_2 ratio		
1:10	472	1
1:5	660	1
1:4	704	2
1:1.6	1046	2
1:0.54	1470	2
1:0	2103	2

thruster in specific impulse. The atomic hydrogen rocket may have other advantages over competing propulsion systems, for interplanetary flight, e.g., the mass driver, the ion drive, and the solar sail, which may allow it to carve out a niche for itself in a performance regime that will be of practical use.

In the late 1950s studies were made of the feasibility of trapping free hydrogen atoms in a solid matrix at 4.2 K.[2] In addition to the technical problems in maintaining the stored atoms at this temperature, to prevent spontaneous recombination, theoretical studies[8] put an upper limit of some 10% on the fraction of atoms in such a matrix. Although Table 1 shows that this might produce an adequate specific impulse, comparable to the best chemical rockets, the technical problems of storage at liquid helium temperatures might produce a mass penalty sufficient to counteract the advantages.

The system currently under study circumvents the latter problems, promising a source of hydrogen atoms efficient enough to be used on board a space vehicle, using the dissociation-recombination cycle to couple energy into the hydrogen working fluid as needed. In the proposed system (Fig. 1), suitable for an interplanetary spacecraft, solar energy would be collected and converted to electricity through solar panels. The electricity would be converted to microwave radiation, and fed into a resonant cavity. Hydrogen, flowing through the cavity, would be ionized, forming a plasma. A significant fraction of the molecules would be dissociated as well, absorbing the energy needed from the microwave radiation. The dissociated hydrogen would flow out of the cavity into a recombination chamber, where it would recombine, releasing the energy absorbed in dissociation as heat and the hot gas would escape out a nozzle to produce thrust.

Thermodynamics and Reactions

The 104.2 kcal/gmole released in the recombination of dissociated hydrogen atoms, besides providing the potential for the high specific impulse of the atomic hydrogen rocket, also produces problems in both engineering and thermodynamics. If one ignores equilibrium considerations, and permits a fully dissociated hydrogen stream to adiabatically and completely recombine, the temperature rise of the gas is in the vicinity of 15,000 K, assuming the specific heat for hydrogen is 7 cal/gmole K. However, Fig. 2 shows that the equilibrium dissociation for hydrogen is over 90% at only 5000 K at 1 atm, and even higher at lower pressures, impelling consideration of equilibrium limitations. Tables 2 and 3 include this consideration, showing the temperature (T) and degree of dissociation (X) for a stream of hydrogen with dissociation X_0 at 300 K, then allowed to reach equilibrium adiabatically, at pressures of 1 atm (Table 2) and 25 atm (Table 3). The specific heat for atomic hydrogen was assumed to be 5 cal/gmole K. The tables also include the specific impulse for each case, assuming frozen flow, no change in composition, through the nozzle. These figures and tables illustrate one of the design problems of a recombination rocket system. In the dissociation section, where recombination should be suppressed, low pressures are desirable. In the recombination zone, high pressures are desired to obtain as much recombination as possible. A suitable compromise pressure, or a design that produces such a reverse pressure gradient, is a goal of the present study.

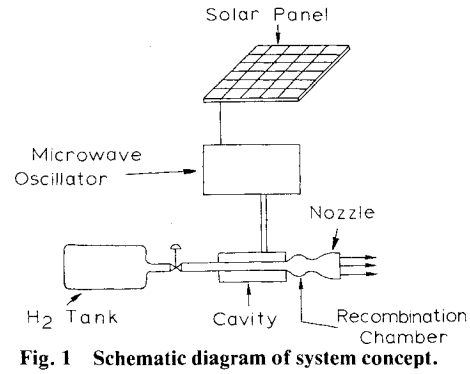

Fig. 1 Schematic diagram of system concept.

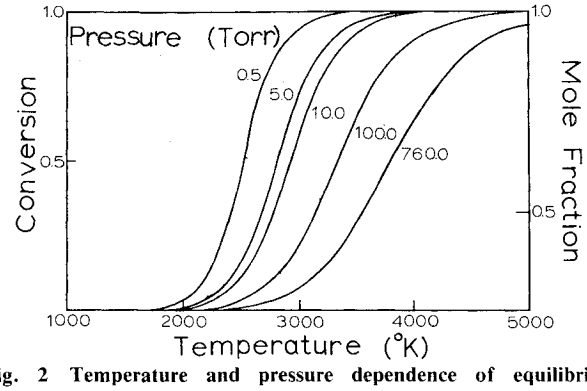

Fig. 2 Temperature and pressure dependence of equilibrium dissociation for H_2.

Table 2 Equilibrium performance of atomic hydrogen rockets inlet temperature 300 K; chamber pressure 1 atm

Fraction inlet	Dissociated outlet	Outlet temperature, K	Specific impulse, s
0.11	0.0008	2000	780
0.16	0.01	2500	880
0.26	0.07	3000	970
0.51	0.27	3500	1100
0.91	0.60	4000	1230
1.00	0.67	4100	1270

Table 3 Equilibrium performance of atomic hydrogen rockets inlet temperature 300 K; chamber pressure 25 atm

Fraction inlet	Dissociated outlet	Outlet temperature, K	Specific impulse, s
0.11	0.0002	2000	780
0.15	0.002	2500	870
0.20	0.015	3000	960
0.28	0.055	3500	1040
0.41	0.15	4000	1130
0.62	0.31	4500	1240
0.90	0.51	5000	1360
1.00	0.59	5200	1400

Within the plasma, four reactions take place:

$$H_2 + e^- \rightarrow 2H + e^- \quad (1)$$

$$H + H_2 + H \rightleftharpoons 2H_2 \quad (2)$$

$$H + H + H \rightleftharpoons H_2 + H \quad (3)$$

$$H \xrightarrow{wall} \tfrac{1}{2}H_2 \quad (4)$$

plus the ion electron reactions characteristic of a plasma. Reaction (1), molecular dissociation by electron impact, is the primary mechanism for dissociation in the plasma as conditions are such that reactions (2) and (3) would be driven to the right, towards recombination. This collisional dissociation involves primarily the interaction between the free electrons and the electrons of the molecule. A collision with a suitable energetic electron can excite the molecular electrons out of their ground ($^1\Sigma_g^+$) state (see Fig. 3), a bonding molecular orbital, into the first excited state ($^3\Sigma_u^+$), an antibonding orbital, and the molecule dissociates.[9] Second, the electron can supply sufficient energy directly to the nuclei to set them vibrating enough to dissociate. Downstream, reactions (2-4) predominate, with the relative importance dependent on the conditions. At high atom concentrations, reaction (3) dominates, with (2) replacing it as recombination proceeds. The rate of reaction (4) is very dependent on the wall materials, and unless the wall material is selected carefully, wall recombination can become the dominant reaction. This would not be preferred in the design system since wall recombination would put much of the energy into the wall. As it would be preferable for the energy to remain in the working fluid, and the transfer of energy from the walls to the gas would be rather inefficient, the wall recombination reaction (4) should be suppressed, allowing the volume recombination reactions (2) and (3) to dominate.

The recombination reactions are three-body reactions for reasons of conservation of energy and of angular momentum. There is also some evidence[10,11] that some of the energy of recombination may become vibrational energy of the recombined molecule. One of the goals of the current study is to determine how much of the recombination energy becomes vibrational energy and how fast the vibrational energy is converted through collisional relaxation to kinetic energy.

Experimental Goals

The experimental phase of the research is designed with several complementary goals in mind. The first is to provide a laboratory scale demonstration of the concept of a microwave plasma-hydrogen atom rocket. The experiments are also to provide the data necessary to verify and rectify the parameters of the mathematical models that are being developed to allow design of such systems on a practical scale. Another goal is to provide a detailed energy balance analysis of the microwave plasma-dissociation-recombination cycle, so that the energy efficiency of the entire concept may be determined so as to compare with competing systems.

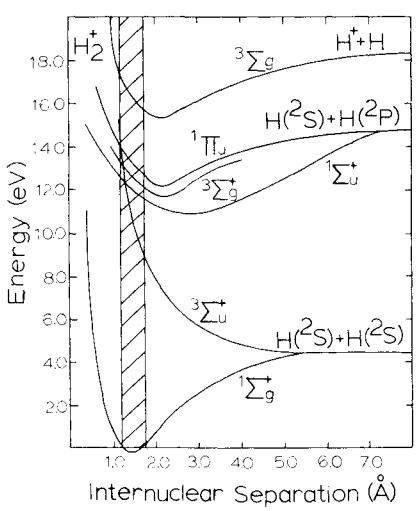

Fig. 3 Molecular energy diagram for hydrogen.

Apparatus

The experimental apparatus, similar to that of Mertz,[6] is described schematically in Fig. 4. A metered stream of 99.9999% hydrogen gas is fed to a 22-mm-i.d. quartz tube concentric with the adjustable length resonant cavity, which is illustrated in Fig. 5. Microwave radiation (2.47 GHz) is coupled to the cavity from a 1.3-kW source through wave guide and coaxial cable. Coupling of the energy results in the breakdown of the low-pressure (100-600 Pa) gas.

Nitrosyl chloride (NOCl) is fed to the gas stream 15 cm from the exit of the discharge region. The titration endpoint is observed optically. The titrant and products of the titration reaction are trapped out of the stream in a liquid nitrogen cold trap.

Fine control of system pressure is maintained by introduction of a variable flow rate commercial grade hydrogen stream between the titrant inlet and vacuum pump inlet.

The microwave frequency signal from the magnetron is attenuated with a variable power divider in line between a three-port circulator and the magnetron. A matched load on the circulator protects the magnetron from high reflected power levels. A directional coupler in line between the circulator and resonant cavity allows measurement of incident and reflected power levels.

A diagnostic mode branch is used to identify empty cavity electromagnetic modes by locating resonant frequencies at low power levels.

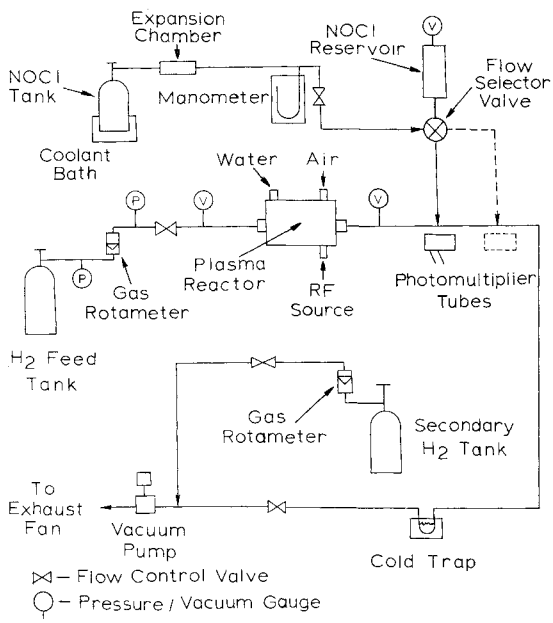

Fig. 4 Flow diagram of process system.

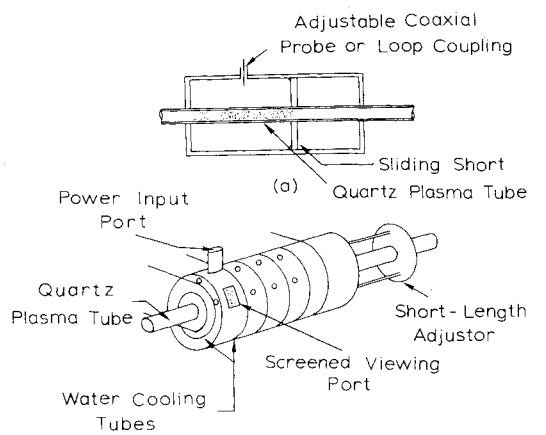

Fig. 5 The plasma cavity: a) cross section, b) external view.

Titration

The reactions involved in the titration are

$$NOCl + H \rightarrow HCl + NO \quad (5)$$

$$H + NO \rightarrow HNO^* \quad (6)$$

$$HNO^* + M \rightarrow HNO + M + h\nu \quad (7)$$

$$H + HCl \rightarrow H_2 + Cl \quad (8)$$

$$Cl + \text{wall} \rightarrow \tfrac{1}{2}Cl_2 \quad (9)$$

$$H + Cl_2 \rightarrow HCl + Cl \quad (10)$$

The rate of reaction (5) is very fast, whereas the rate of reaction (6) is much slower. As the titration proceeds, the NOCl flow rate is increased and the HNO* emission monitored. The "endpoint" for the titration scheme is when the HNO* emission is just extinguished. At this point and for these conditions, reaction (5) is the only reaction occurring and is stoichiometric; i.e., the molar flow rate of atomic H is equal to that of NOCl. After the "endpoint" is determined, the NOCl flow is then diverted from the flow system to the reservoir and measured, yielding the atomic H flow rate.

The photon produced in reaction (7), the relaxation of the excited HNO* molecule, has one of several wavelengths between 6300 and 7500 Å.[12] A long pass filter that has a cutoff of 6350 Å is used in conjunction with a photomultiplier tube (PMT) that has an upper detection limit of 7500 Å, to monitor the HNO* emission.

Reducing the surface recombination coefficient for atomic Cl to less than 10^{-4} forces the equilibrium of reaction (9) to the left. This factor, along with the presence of excess H_2, then forces the equilibrium of reaction (8) to the left. Also if reaction (9) does not proceed, then it is obvious that reaction (10) cannot proceed either.

The surface coating used to decrease surface recombination was a commercially available mixture of di- and tri-chloro silanes. It was found that the silane polymer coating strongly absorbed in the region of the HNO* emission and a window coated with ortho-phosphoric acid was inserted at the titration inlet to facilitate the HNO* emission detection.

The sensitivity of the NOCl flow control was increased by maintaining the NOCl at −30 K by a dry ice/ethylene glycol/water bath and reducing its vapor pressure to 180 Torr (2.4×10^4 Pa).

Calculations and Definitions

The measure of the dissociation, the conversion (X), of molecular to atomic hydrogen is defined in Table 4 and is calculated from the NOCl and initial molecular hydrogen flow rates.

$$X = F_H/2F_{H_2} = F_{NOCl}/2F_{H_2} \quad (11)$$

The NOCl flow rate is determined, assuming ideal gas behavior, by a linear least-squares fit of the pressure rise in a constant volume reservoir with the regression coefficients of the linear fit always exceeding 0.995.

$$F_{NOCl} = \frac{dn}{dt} = \frac{dP}{dt}\frac{V}{RT} = F_H \quad (12)$$

Incident and reflected power levels are measured at the directional coupler and give the total power absorbed by the plasma cavity system. The average power density is defined as total power absorbed divided by the plasma volume. In calculating the plasma volume, the plasma is assumed to fill the entire cross section of the quartz discharge tube. However, the center of this cross section appears to be plasma-free and the size of the plasma-free area varies with experimental conditions.

Table 4 Stoichiometric table[a]

Species	Molar flow rate in	Molar flow rate out	Mole fraction	Molar concentration
H_2	F_{H_2}	$(1-X)F_{H_2}$	$\frac{1-X}{1+X}$	$\frac{1-X}{1+X}\frac{P}{RT}$
H	0	$2XF_{H_2}$	$\frac{2X}{1+X}$	$\frac{2X}{1+X}\frac{P}{RT}$
Total	F_{H_2}	$(1+X)F_{H_2}$	1.0	$\frac{P}{RT}$

[a] Where X is the conversion (dissociation) of one mole of molecular hydrogen (H_2) to two moles of atomic hydrogen (H); F_{H_2} is the initial molar flow rate of H_2; and ideal gas behavior assumed.

Results and Discussions

The experimentally measured conversions as a function of flow rate at a constant pressure and power density are given in Figs. 6 and 7. These conversions are measured 15 cm downstream from the exit of the discharge. At low pressures, model predictions show that the hydrogen atom concentrations will decrease only slightly over this distance. As can be seen in Figs. 6 and 7 and supported by other data, the conversion of molecular to atomic hydrogen increases with flow rate and power density, and decreases with pressure.

Curves A and B of Fig. 6 represent two reproducible steady states dependent on the initial conditions. Curve A results when rf power is applied to the evacuated cavity followed by the introduction of the gas stream and pressure increased to the operating conditions. Curve B results when the desired operating pressure is first attained and then the rf power is applied. Theoretical work has established a basis for bifurcating solutions of the nonisothermal dispersion model equations.

The plasma cavity is always tuned for an optimum power match, i.e., minimum reflected power, by adjusting the sliding short length and probe depth (see Fig. 5). The optimum power match was found to be critically dependent on the system pressure but not on the flow rate. As the cavity was tuned toward an optimum power match, the discharge was more susceptible to instabilities related to perturbations and it was increasingly difficult to maintain a steady-state discharge. As the pressure was increased from 1 to 5 Torr (133 to 665 Pa), the plasma length and the intensity of the discharge emission decreased, the size of the plasma free center increased, and small changes in sliding short length and probe depth were not as critical. An increase in the pressure also required a decrease in the sliding short length and an increase in the probe depth to maintain an optimum power match.

Periodic variations in the emission intensity were observed along the discharge. Transient behavior on the order of a few minutes was observed when the plasma was ignited, which indicates the importance of the initial conditions on the steady-state operation. During this initial period, the color of the discharge emission progressed from a more intense red to a less intense violet and the measured incident power increased or decreased approximately 10%, depending on the initial condition. Unfortunately, the intense emission from the discharge corresponds to the same wavelengths as the HNO* emission, interfering with the optical endpoint detection.

From studies done on the eigen modes of this cavity system, the TE^*_{011} and TM^*_{111} modes have intersecting solutions in the operating region of interest. Plots of normalized absorbed power vs collision frequency for momentum transfer normalized with the driving frequency show a maximum at 3.2 Torr or 427 Pa. This calculation, derived from the Langevin equation, assumes a momentum transfer collision frequency of $4.85 \times 10^9 \times P$ (P in Torr) or $3.64 \times 10^7 \times P$ (P in Pascals).

The operating pressures of this investigation bracket this maximum.

The ratio of the power absorbed in the dissociation of the hydrogen molecules to the total power absorbed by the plasma cavity system increases with increasing flow at a constant pressure. It is expected that this power ratio will reach a maximum.

Important plasma parameters are listed in Table 5. Values of these parameters were estimated based on representative results of previous investigations and are tabulated in Table 5 along with results from this work.

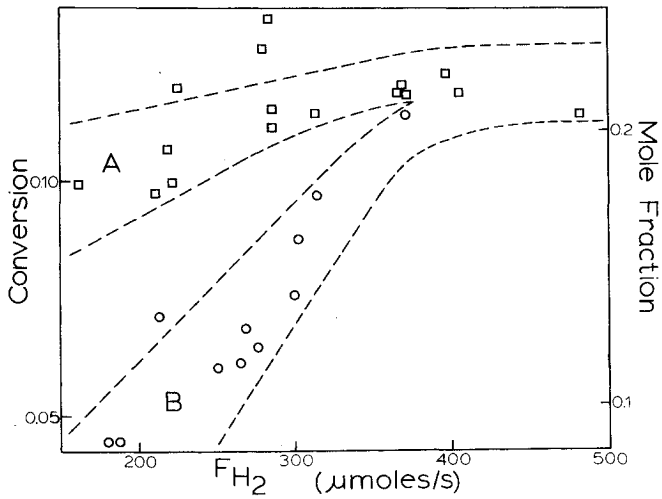

Fig. 6 Dissociation of molecular hydrogen as a function of flow rate at 2.7 Torr.

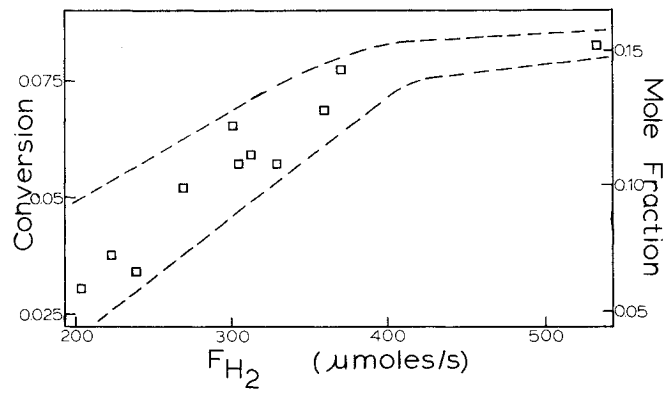

Fig. 7 Dissociation of molecular hydrogen as a function of flow rate at 4.1 Torr.

Modeling

Optimization of the hydrogen atom generation and recombination for thrust production requires consideration of the discharge zone and of the recombination reactions and nozzle characteristics of the downstream zone. Plasma zone modeling is an attempt to correlate plasma properties to the species and energy distributions at the outlet of the plasma zone. The downstream modeling is an analysis of the energetics of the recombination reactions.

Modeling of the Plasma Zone

Modeling of the plasma zone considers mixing, reaction pathways and time scales for energy transfer between reactive species in a nonisothermal flowing system. Mixing in the discharge zone is treated by consideration of the limiting cases of plug flow and a well mixed condition in the reaction zone. The reaction pathways include dissociation through direct impact and vibrational excitation processes, three body gas phase recombination reactions, and surface catalyzed recombination reactions. A detailed energy balance is developed to account for the nonisothermal nature of the plasma discharge.

The time scales of the excitation, relaxation, and transport processes occurring in a low-pressure (3-Torr/400-Pa) microwave discharge in hydrogen vary widely in magnitude but may be grouped in several ranges. The shortest scale is that of electron H_2 interaction, with an intercollisional time of 5.0×10^{-11} s. Binary molecular and atomic intercollisional times are on the order of 1.0×10^{-7} s and H_2-H exchange V-T relaxation times are on the order of 1.0×10^{-4} s . Atomic recombination, H_2-H_2 V-T relaxation and flow stream residence time scales are on the order of 0.01-1.0 s.

There is a marked difference between the time scales for randomization of energy among the vibrational states and that for relaxation to a distribution characterized by the molecular kinetic temperature. To a first approximation, it is

Table 5 Results of hydrogen radical generation experiments

Worker	Mearns and Ekinci[18]	Shaw[4]	Poole[19-21]		This investigation
Experimental conditions					
Pressure, Pa/Torr	133/1.0	66.7/0.5	100/0.75	56.0/0.42	360./2.7
Initial molecular hydrogen flow rate, g mole/s	1.4×10^{-4}	1×10^{-5}	9.8×10^{-5}	9.6×10^{-5}	$(1.8\text{-}4.8)\times10^{-4}$
Power absorbed, W	85	100	47.5	49.5	380
Dimensions					
Discharge tube i.d., mm	11	8	25		22
Discharge length, cm	12	7	54		12.5
Plasma volume, cm	11.4	~2.5	264		47.5
Surface coating	H_3PO_4	Dri-film	H_3PO_4		Dri-film
Discharge characteristics					
Driving frequency, MHz	2450	3000	dc	dc	2470
Average power density, W/cm	7.5	40	0.18	0.19	8.2
PA, (Pa-cm)/(Torr-cm)	21.33/0.16	11.07/0.083	52.00/0.39	29.33/0.22	165/1.24
E/P, (V/cm-Pa)/(V/cm-Torr)	0.28/37	0.13/17	0.19/25	9.23/30	0.24/33
Plasma space time, s	4.38×10^{-3}	6.72×10^{-3}	1.09×10^{-1}	6.21×10^{-2}	$(3.83\text{-}1.44)\times10^{-2}$
Atomic hydrogen flow rate, g mole/s	1.064×10^{-4}	1.8×10^{-5}	1.5092×10^{-5}	4.435×10^{-5}	$(1.2\text{-}10.)\times10^{-5}$
Conversion, %	38[a]	90[a]	7.7[a]	23.1[a]	3.4-14
Yield,[b] g moles of atoms/KWh	4.506	0.6480	1.144	3.226	0.1137-0.9474
Molecular hydrogen flow rate for 1 lb thrust, g mole/s	0.1729	0.1124	0.3842	0.2218	0.5782-0.2849
Scale factor, (1 lbf thrust flow/exp flow)	1200	11,200	3900	2400	3200-600
P_{Diss}/P_{abs},[c] dimensionless	0.2729	0.03924	0.06926	0.1953	0.0070-0.0771

[a] Unclear as to whether measured and where or extrapolated to in plasma. [b] Thermodynamic upper limit of the yield is 16.6 g moles of atoms/KWh based on dissociation energy of 104.2 K cal/g mole. [c] Ratio of the power absorbed in the dissociation of hydrogen to the total power absorbed by the plasma cavity system.

assumed that the distribution of diatomics over the vibrational levels is characterized by a single vibrational temperature. Through an energy balance over the vibrational states, the rates of excitation, relaxation, and depopulation of excited states by chemical reaction are related. With the energy balance over the vibrational states, the thermal energy balance, assumption of constant total pressure, and a mass balance on the diatomic, one further relation is required to specify the state of the system. A relation between excitation rates and the excitation field strength is found by an expansion of the Boltzmann equation. A solution of the Boltzmann equation describes in detail the time evolution of the distribution of the electron gas over possible energies and positions. A two term expansion of the Boltzmann equation in spherical harmonics in velocity space is used to relate electric field strength to inelastic processes resulting in vibrational excitation and dissociation.

Two transport models are used, the well mixed reactor model (C^*) and the plug flow reactor model (PFR). The time scale for mixing in the well mixed reactor model is much smaller than that for the other processes so no gradients of temperature or species concentration exist. The PFR model assumes "plug"' flow through a tubular reactor with axial transport by convection only. Nonlinear transport and kinetic terms result from the dissociation of the diatomic and these terms are retained in the model equations.

A numerical simulation by the method of orthogonal collocation was done and sample predictions of conversion of molecular hydrogen to atomic hydrogen, evaluated at the reactor exit, are plotted in Fig. 8.

As predicted from the relative time scale of atomic recombination and gas flow, atomic recombination processes do not control the behavior of the discharge. In Fig. 8, predicted conversions from the two transport models are given. The upper curve is the conversion predicted by the PFR model, the lower curve is that of the C^* model. Numerical simulations with both models indicate that inelastic electron energy loss rates to the diatomic molecule and vibrational to translational energy transfer rates are the principal determinants of the predicted conversion. The curves in Fig. 8 are calculated with V-T relaxation rate coefficients reported by Audibert et al.[13,14] and Heidner and Kaspar.[15] Numerical simulations also indicate that as the time scale for V-T relaxation processes becomes small with respect to species residence time, the results of the PFR model approach those of the C^* model. Predicted conversions also point out the importance of mixing effects for low rates of V-T relaxation processes, or high flow rates.

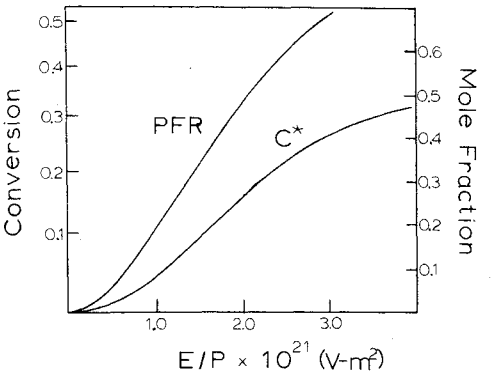

Fig. 8 Comparison of PFR and C^* transport model predictions.

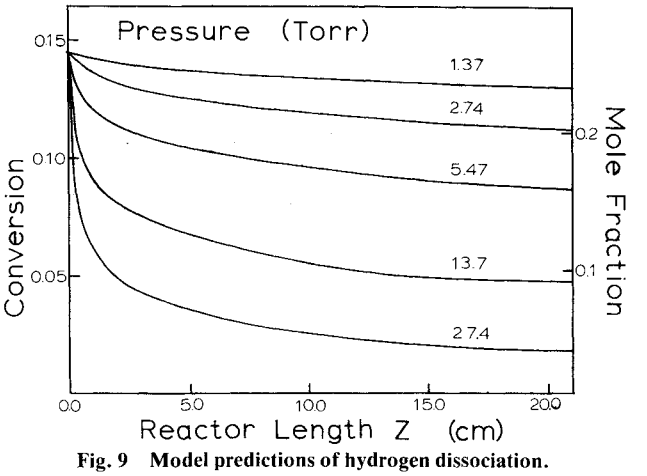

Fig. 9 Model predictions of hydrogen dissociation.

Table 6 Parameters of modeled run

Experimental parameters	
Hydrogen feed rate	3.163×10^{-7} kg mole/s
Inside diameter of reaction volume	2.2 cm
System pressure at titration point	2.74 Torr/364.9 Pa
Position of titration point	15.3 cm
Measured dissociation, %	0.11482
Model parameters	
Initial dissociation	0.145
Initial temperature (assumed)	300 K

Modeling of the Recombination Zones and Nozzle

The recombination zone and nozzle are modeled as a one-dimensional plug flow reactor. This model is used to predict axial variation of pressure, temperature, and composition conditions. Applying material and energy balances to a differential length (Δz) of the recombination zone gives the following differential equation:

$$\frac{dX}{dz} = \frac{\Re A}{F_{H_2}} \tag{13}$$

$$\frac{dT}{dz} = -\left[\frac{m_0 u_b^2}{g_c T}\left(\frac{1}{(1+x)}\frac{dX}{dz} - \frac{1}{A}\frac{dA}{dz}\right) - \Delta H(T)\frac{dx}{dz}\right] \Big/ \left(\frac{m_0 u_b^2}{g_c T} + c_p(T,X)\right) \tag{14}$$

where $\Re$ is the rate of dissociation, given by

$$\Re = (k_1[H] + k_2[H_2])([H_2] - K_{eq}[H]^2) - k_{wall}[H] \tag{15}$$

The model equations, with appropriate constants, are solved numerically via a standard, two-dimensional, fourth-order Runge-Kutta method. The rate constants for volume recombinations as functions of temperature were derived from a least-squares fit to the data of Shui and Appleton[16] (hydrogen molecule as third body) and Shui[17] (hydrogen atom third body) to a convenient three parameter form:

$$k(T) = aT^b e^{-c/T} \tag{16}$$

For hydrogen atoms as a third body, the rate constant is proportional to $T^{-0.72}$, and for molecules as third body, the rate constant depends on $T^{-0.75}$, with small activation energies, $C = 20$ and 92 K, respectively. The equilibrium constant was calculated as a function of temperature by use of published relationships between heat capacities and temperature.

The modeling is applied to a constant area and constant pressure system. At low pressures in properly coated tubes, wall recombination is neglected. As the pressure increases, much more of the dissociated atoms recombine early in the recombination zone before the rate tapers off owing to approaching equilibrium and the strong temperature dependence of the reaction rate.

Conclusions

Over 120 experiments were conducted to dissociate hydrogen flowing through a microwave plasma for pressures from 1 to 5 Torr (133 to 665 Pa) and flow rates of hydrogen from 100 to 500 μmole/s. Conversions of molecular to atomic hydrogen were measured at a point 15 cm downstream from the plasma outlet using NOCl titration, resulting in conversions ranging between 5 and 15% with corresponding mole percents of atomic hydrogen of from 10 to 25. Average power density in the plasma varied between 5 and 13 W/cm^3.

Cavity tuning, discharge stability, and optimum power coupling are critically dependent on the system pressure but are nearly independent of the flow rate. Measured conversions increased with flow rate and power density, but decreased with pressure. Since hydrogen atom concentrations were measured 15 cm downstream from the plasma outlet, the fact that the conversion increased with increasing flow rate suggests that hydrogen atom conversion in the plasma is a weak function of residence time in the plasma and depends mainly on the residence time between the plasma outlet and the titration point.

The effect of pressure on these measured downstream conversions may be due to an increase in gas phase atomic recombination losses with increasing pressures. These trends for the dependence of conversion on flow rate, power density, and pressure are consistent with models of the complex transport and kinetic processes which occur in both the plasma and downstream recombination regions.

The duration of the observed transient period preceding steady-state operation is large in comparison with the time scale of the processes taking place in the discharge and indicates a possible effect of initial conditions on the steady-state behavior of the discharge.

Acknowledgments

The authors acknowledge the support of NASA Lewis Research Center, Contract NSG-3299, in this research and the work of David Ball, who prepared much of the experimental data for computer analysis.

References

[1] Palmer, E.B., "Burning Rate of an H-Atom Propellant," *ARS Journal,* Vol. 29, 1959, pp. 365-366.

[2] Stewart, P.A.E., "Liquid Hydrogen as a Working Fluid in Advanced Propulsion Systems," J.B.I.S., Vol. 8, 1962, pp. 225-240.

[3] Sutherland, G.S., "Recent Advances in Space Propulsion," *ARS Journal,* Vol. 29, 1959, pp. 698-705.

[4] Shaw, T.M., "Dissociation of Hydrogen in a Microwave Discharge," *Journal of Chemical Physics,* Vol. 30, 1959, p. 1366.

[5] Malavarpu, R., Asmussen, J., and Hawley, M.C., "Behavior of a Microwave Cavity Discharge Over a Wide Range of Pressures and Flow Rates," *IEEE Transactions on Plasma Science,* Ps-6, Vol. 4, Dec. 1978, p. 341.

[6] Mertz, S.F., Asmussen, J., and Hawley, M.C., "A Kinetic Model for the Reactions of CO and H_2 to CH_4 and C_2H_2 in a Flow," *IEEE Transactions on Plasma Science,* OS-4, Jan. 1976, p. 11.

[7] Sutton, G.P. and Ross, D.M., *Rocket Propulsion Elements,* 4th ed., Wiley and Sons, New York, 1976.

[8] Golden, B., "Free Radical Stabilization in Condensed Phases," *Journal of Chemical Physics,* Vol. 29, 1958, pp. 61-71.

[9] Snellenberger, R.W., "Hydrogen Atom Generation and Energy Balance," M.S. Thesis, Michigan State University, East Lansing, Mich., 1981.

[10] Villermaux, J. and Gilbert, R., "Production of Molecular Hydrogen in an Elevated Vibrational State by Homogeneous Recombination of Atomic Hydrogen," *Compte Rendu,* Vol. 255, 1962, p. 690.

[11] Levitskii, A.A. and Polak, L.S., "Study of the Recombination Reactor $H+H+H \rightarrow H_2+H$ by the Classical Trajectories Method," *Khimiya Vysokikh, Energii,* Vol. 12, 1973, p. 291.

[12] Bancroft, J.L., Holeas, J.M., and Ramsay, D.A., "The Absorption Spectra of HNO and DNO," *Canadian Journal of Physics,* Vol. 40, 1962, pp. 322-346.

[13] Audibert, M.M., Jaffrin, C., and Ducuin, J., "Vibrational Relaxation of Molecular Hydrogen in the Range 40-500°K," *Chemical Physics Letters,* Vol. 25, Feb. 1974, pp. 156-163.

[14] Audibert, M.M., Viloseca, R., Rukasit, J., and Ducuin, J., "Vibrational Relaxation of Ortho- and Para-Hydrogen in the Range of 400-500°K," *Chemical Physics Letters,* Vol. 31, Feb. 1975, pp. 232-233.

[15] Heidner, R.F. III and Kasper, J., "Experimental Rate Constant for $H+H_2$ ($v''=1$) $H+H_2$ ($v''=0$)," *Chemical Physics Letters,* Vol. 15, Feb. 1972, pp. 179-189.

[16] Shui, V.H. and Appleton, J.P., "Gas-Phase Recombination of Hydrogen. A Comparison Between Theory and Experiment," *Journal of Chemical Physics,* Vol. 55, 1971, pp. 3126-3132.

[17] Shui, V.H., "Thermal Dissociation and Recombination of Hydrogen According to the Reactions $H_2+H \rightleftharpoons H+H+H$," *Journal of Chemical Physics,* Vol. 58, 1973, p. 4868.

[18] Mearns, A.M. and Ekinci, E., "Hydrogen Dissociation in a Microwave Discharge," *Journal of Microwave Power,* Vol. 12, 1977, p. 156.

[19] Poole, H.G., "Atomic Hydrogen. I. Calorimetry of Hydrogen Atoms," *Proceedings of the Royal Society of London,* Vol. A163, 1937, p. 404.

[20] Poole, H.G., "Atomic Hydrogen, II. Surface Effects in the Discharge Tube," *Proceedings of the Royal Society of London,* Vol. A163, 1937, p. 415.

[21] Poole, H.G., "Atomic Hydrogen. III. The Energy Efficiency of Atom Production in a Glow Discharge," *Proceedings of the Royal Society of London,* Vol. A163, 1937, p. 424.